Appl Compos Mater
DOI 10.1007/s10443-013-9374-z

# Optimization and Reliability Analysis of 2.5D C/SiC Composites Turbine Stator Vane

**Zhigang Sun · Chunyuan Kong · Xuming Niu · Yingdong Song · Xianqiao Wang**

Received: 9 December 2013 / Accepted: 12 December 2013


**Abstract** This paper presents a feasible and efficient methodology to design 2.5D C/SiC composites vane system. To better represent the architecture of 2.5D C/SiC composites, here we define five geometric parameters to describe its microstructure based on the optical photomicrographs. The double scale model for mechanical properties of 2.5D C/SiC composites has been presented to provide a reliable validation with the experimental results. Meanwhile, Monte Carlo (MC) simulation method has been employed to investigate the stochastic behavior of 2.5D C/SiC composites mechanical properties. MC simulation results show that mechanical properties of 2.5D C/SiC composites heavily depends on the stochastic behavior of components and the microstructure of 2.5D composites. To fully explore the potential of 2.5D C/SiC composite, finally we present a vane optimization model and investigate its reliability by integrating the analytical model for mechanical properties with the finite element model analysis. These findings provide an effective method to assess the risk of vane design.

**Keywords** 2.5D C/SiC composites · Optimization · Reliability analysis · Mechanical properties · Safety factor

## 1 Introduction

Owing to its high strength and toughness, composite materials have enjoyed the great popularity in a variety of applications, such as structural materials for aerospace industry, internal chambers and thermal components in aircraft engine [1]. To broaden the full potentiality of composite materials, optimal design has been employed to maximize its material properties, especially in laminated composite. Kim [2] developed a kind of optimal method for tapered composite laminates by taking into account the discrete ply angles and the number of

Z. Sun (✉) · C. Kong · X. Niu · Y. Song
College of Energy and Power Engineering and Jiangsu Province Key Laboratory of Aerospace Power System, Nanjing University of Aeronautics and Astronautics, Nanjing, People's Republic of China 210016
e-mail: szg_mail@nuaa.edu.cn

X. Wang
College of Engineering, University of Georgia, Athens, GA 30602, USA

Published online: 11 January 2014

plies in each patch. Liu [3] maximized the buckling load of laminate with discrete ply angles by utilizing standard genetic algorithms(GA) and permutation GA. Zhao [4] proposed two-level layout optimization strategy for large-scale composite wing structures. By considering the uncertainty of parameters, Eamon [5] combined the analysis reliability with sizing optimization methodology to investigate composite advanced submarine sail structure.

Ceramic composites, as one of the outstanding composites, have been plagued by the unpredicted micro-crack of matrix and unstable thermal-mechanical properties. Puglia [6] demonstrated that defects of ceramic composites such as microcracks and voids from the process of manufacture or service are introduced as a result of the mismatch thermal-mechanical properties of constituent materials. However, owing to their high stiffness and high strength at critical temperature, ceramic-matrix composites (CMCs) are promising materials for engineering applications at extreme conditions [7]. Recent years have witnessed the explosive growth of interest in woven ceramic composites since these materials provide an integrated advantage with high strength, high stiffness, and extraordinary wearability with a non-brittle stress-strain behavior at the extreme conditions [8]. 2.5D composites has shown a more effective way to sustain the system than 3D structure textile composites based on its unprecedented mechanical properties [9]. Until now research for weave structure CMCs are mainly focused on analytical model or testing their mechanical properties. Chang [8] proposed a micro-mechanical model for elastic behavior of angle-interlock woven ceramic composites, and discussed the relationship between its parameters of micromechanical model and its elastic behavior. Ma [10] created a geometric model of 2.5D C/SiC composites, and tested the strength along the warp and weft directions. However, limited endeavor has been devoted to develop a kind of structure design method for 2.5D C/SiC composites, which can combine analytical model of mechanical properties and structure design, reliability analysis together. In this paper, optimization and reliability analysis method will be employed to design 2.5D C/SiC composites turbine stator vane, by integrating analytical model for mechanical properties prediction of 2.5D C/SiC composites with thermal-structure analysis of turbine stator vane.

## 2 Theoretical Analysis of 2.5D C/SiC Composites

### 2.1 Structure of 2.5D C/SiC composites

The microstructure of 2.5D C/SiC composites is obtained from optical photomicrographs. Figure 1 shows a typical photograph of 2.5D C/SiC composites. It can be seen that the warp

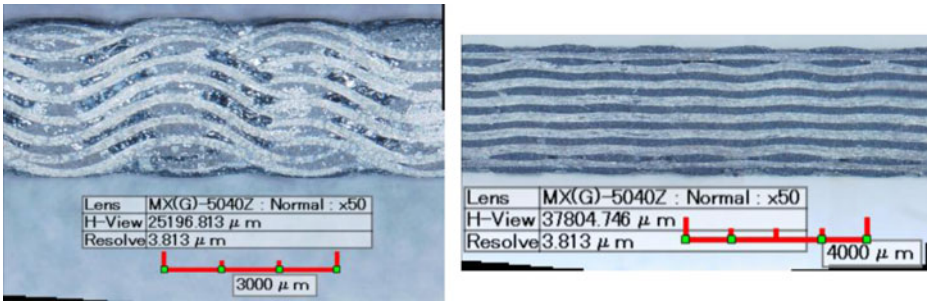


(a) cross-section of weft (b) cross-section of warp

**Fig. 1** Cross-section of 2.5D C/SiC composites **a** cross-section of weft **b** cross-section of warp

yarn is undulating and the weft yarn is straight. There are many regular micro-pores between adjacent yarns. The undulated yarn is coined as warp and the straight yarn is weft.

Figure 2 depicts the typical architecture of 2.5D C/SiC composites. To better describe its microstructure, five distinct parameters are defined as: $J_s$ is the span of warp, $J_h$ is the height of warp, $J_w$ is the width of warp, $W_h$ is the height of weft, and $W_w$ is the width of weft.

The material properties of the microstructure shown in Fig. 2 have a variation along the tow curve. Therefore, when creating the finite element model of the microstructure the material properties of each element in the model are determined by their locations and degrees of undulation. The warp can be considered as a sinusoidal function [11], therefore longitudinal direction of warp in front part and back part can be defined as $\theta_1$ and $\theta_2$:

$$\theta_1 = \arctan\left[(J_h + W_h)\frac{2\pi}{J_s}\sin\left(\frac{2\pi X}{J_s}\right)\right] \tag{1}$$

$$\theta_2 = \arctan\left[-(J_h + W_h)\frac{2\pi}{J_s}\sin\left(\frac{2\pi X}{J_s}\right)\right] \tag{2}$$

where, $\theta_1$ is the angle between the front part of warp and the x axis; $\theta_2$ is the angle between the back part of warp and the x axis; $X$ means the value of x axis.

Figure 3a shows the finite element model of 2.5 C/Sic composites microstructure, in which direction 1 is the direction of warp, and direction 3 is the direction of weft. Figure 3b and c show the longitudinal direction of front part and back part of the warp, respectively.

## 2.2 Elastic Properties and Thermal Expansion Coefficient

Here an iso-strain assumption is employed to present the theoretical models for elastic properties and thermal expansion coefficient (TEC). The equivalent stiffness matrix of the material can be expressed as follow:

$$\overline{\mathbf{C}}_{ijkl} = \sum_{k=1}^{N} v^{(k)}\left(\mathbf{T}'\mathbf{C}'^{(k)}_{ijkl}\mathbf{T}\right) \tag{3}$$

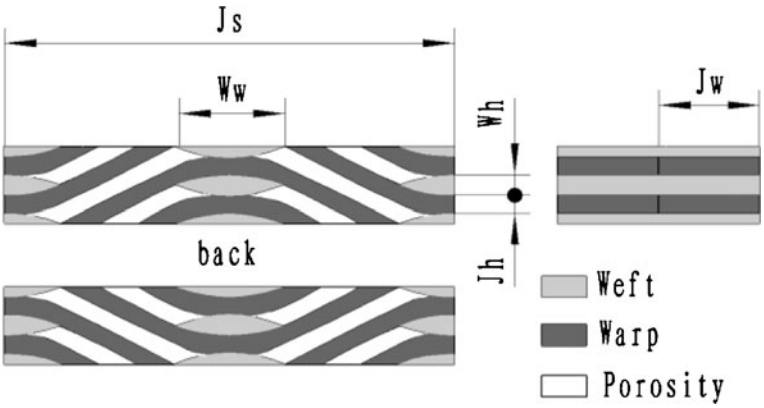


**Fig. 2** Microstructure of 2.5D C/SiC composite

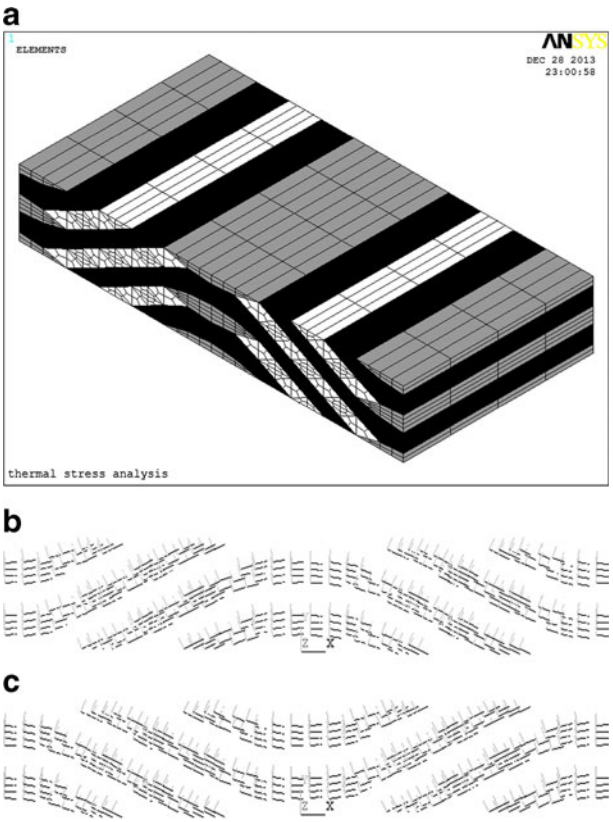


**Fig. 3** Finite element models of 2.5D C/SiC composites **a** Finite element model of 2.5D composites **b** Longitudinal direction of front part **c** Longitudinal direction of back part

Similarly, the equivalent thermal expansion coefficient is termed as:

$$\overline{\alpha}_{kl} = \overline{C}^{-1}_{ijkl} \sum_{k=1}^{N} v^{(k)} \left( \mathbf{T}' \mathbf{C}'^{(k)}_{ijkl} \alpha^{(k)}_{kl} \right) \tag{4}$$

Where, $\overline{C}_{ijkl}$ and $\overline{\alpha}_{kl}$ denote the average stiffness matrix of composite, $\mathbf{C}'^{(k)}_{ijkl}$ and $\boldsymbol{\alpha}^{(k)}_{kl}$ denote the stiffness matrix and thermal expansion coefficient of the No. k component, $v^{(k)}$ is the volume fraction, $\mathbf{T}'$ is transfer matrix between the global coordinate system and the local coordinate system, defined in Eq. (9), N is the components number.

In the micro-scale, the material direction of components in the global coordinate system is the same as local coordinate system. Therefore, the stiffness matrix and the thermal expansion coefficient in the micro-scale are expressed as follow:

$$\overline{\mathbf{C}}^{micro}_{ijkl} = v^{(f)} \mathbf{C}^{(f)}_{ijkl} + v^{(m)} \mathbf{C}^{(m)}_{ijkl} \tag{5}$$

$$\overline{\alpha}_{kl}^{micro} = \overline{C}_{ijkl}^{-1}\left(v^{(f)}C_{ijkl}^{(f)}\alpha_{kl}^{(f)} + v^{(m)}C_{ijkl}^{(m)}\alpha_{kl}^{(m)}\right) \tag{6}$$

where, $\overline{C}_{ijkl}^{micro}$ is the equivalent stiffness matrix of the fiber tow, $\overline{\alpha}_{kl}^{micro}$ is the equivalent thermal expansion coefficient of the fiber tow, $v^{(f)}$ is the fiber volume fraction, $C_{ijkl}^{(f)}$ is the stiffness matrix of fiber, $\alpha_{kl}^{(f)}$ is the TEC of fiber, $v^{(m)}$ is the matrix volume fraction, $C_{ijkl}^{(m)}$ is the stiffness matrix of matrix, $\alpha_{kl}^{(m)}$ is the TEC of matrix, because of porosity existing in micro-scale [6, 7], $\mathbf{v^{(f)}+v^{(m)}}$ should less than 1.

In the meso-scale, the material direction of warp has a certain angle between global coordinate system and local coordinate system. The value of the angle can be calculated based on Eqs. (1) and (2). Then, the stiffness matrix and the thermal expansion coefficient in meso-scale are defined as follow:

$$\overline{C}_{ijkl}^{meso} = \sum_{k=1}^{N} v^{(k)}\left(\mathbf{T}'\overline{C}_{ijkl}^{micro}\mathbf{T}\right) \tag{7}$$

$$\overline{\alpha}_{kl}^{meso} = \left(\overline{C}_{ijkl}^{meso}\right)^{-1}\sum_{k=1}^{N} v^{(k)}\left(\mathbf{T}'\overline{C}_{ijkl}^{micro}\alpha_{kl}^{(k)}\right) \tag{8}$$

where, $v^{(k)}$ is volume fraction of element, $\mathbf{T}'$ is the transformational matrix

$$\mathbf{T} = \begin{bmatrix} l_1^2 & m_1^2 & n_1^2 & 2m_1n_1 & 2n_1l_1 & 2l_1m_1 \\ l_2^2 & m_2^2 & n_2^2 & 2m_2n_2 & 2n_2l_2 & 2l_2m_2 \\ l_3^2 & m_3^2 & n_3^2 & 2m_3n_3 & 2n_3l_3 & 2l_3m_3 \\ l_2l_3 & m_2m_3 & n_2n_3 & m_2n_3+m_3n_2 & n_2l_3+n_3l_2 & l_2m_3+l_3m_2 \\ l_3l_1 & m_3m_1 & n_3n_1 & m_1n_3+m_3n_1 & n_1l_3+n_3l_1 & l_1m_3+l_3m_1 \\ l_1l_2 & m_1m_2 & n_1n_2 & m_1n_2+m_2n_1 & n_1l_2+n_2l_1 & l_1m_2+l_2m_1 \end{bmatrix} \tag{9}$$

The cosine of the warp direction is shown as follow:

$$l = \left[\cos\left(\theta^{(k)}\right), \sin\left(\theta^{(k)}\right), 0\right], m = \left[-\sin\left(\theta^{(k)}\right), \cos\left(\theta^{(k)}\right), 0\right], n = [0, 0, 1]$$

The cosine of the weft direction is shown as follow:

$$l = [0, 0, 1], m = [0, 1, 0], n = [1, 0, 0].$$

### 2.3 Material Strength

The failure probability of the fiber [12] in microstructure can be predicted by Weibull analysis with the expression

$$P_f = 1-\exp\left(-\left(\frac{\sigma}{\sigma_c}\right)^{m_f}\right) \tag{10}$$

where, $P_f$ is the probability distribution, $\sigma_c$ is the characteristic strength and $m_f$ is the Weibull modulus, $\sigma$ is the stress in the fiber.

Ultimate strength and failure strain [13] is defined as follow

$$\sigma_{fs} = v_f \sigma_c \left[ \left( \frac{2(m_f + 1)}{(m_f + 2)m_f} \right)^{1/(m_f+1)} \left( \frac{m_f + 1}{m_f + 2} \right) \right] \tag{11}$$

$$\varepsilon_{fs} = \frac{\sigma_c}{E_f} \left[ \left( \frac{2(m_f + 1)}{(m_f + 2)m_f} \right)^{1/(m_f+1)} \right] \tag{12}$$

where, $\sigma_{fs}$ is the ultimate strength, $v_f$ is the fiber volume fraction, $\varepsilon_{fs}$ is the failure strain, $E_f$ is the elastic properties along fiber axis.

Stress-strain curve due to the fiber deformation can be described as in reference [12]

$$\sigma(\varepsilon) = \frac{v_f \sigma_{fs}^{m_f+1}}{(E_f \varepsilon)^{m_f}} \left( 1 - \exp\left( - \frac{(E_f \varepsilon)^{m_f+1}}{\sigma_{fs}^{m_f+1}} \right) \right) \tag{13}$$

The warp and weft elements are treated as laminated composites, using Eqs. (11), (12), and (13) as well as finite element model shown in Fig. 3. Following the iso-strain assumption, we can calculate the average material strength.

The micro stress-strain field of unit cell model can be calculated by ANSYS software, we can obtain the strain of each element under itself principle direction, substitute it in to Eq. (13) to calculate the descending elastic modulus, then re-substitute the descending elastic modulus into unit cell model, iterative calculate until the results become convergent, finally, we can obtain the average stress and strain. Then re-calculate under different periodicity boundary condition until the stress or strain of warp yarns element is higher than the ultimate stress or strain of fiber tows. By this way, we can obtain the stress-strain relationship of unit cell model and the failure mechanical properties of composite.

### 2.4 Comparison of the Theoretical and Experimental Results

To better make comparisons, we utilize the following parameters for our composite models: the fiber volume fraction in the tow is 59.5 %; the porosity in micro scale is 4 %; and the matrix volume fraction is 37.5 %. Also the material properties of each component phase are summarized in Table 1.

**Table 1** Material property for the composite phases

| | $E_L$/GPa | $E_T$/GPa | $G_L$/GPa | $G_T$/GPa | $\alpha_L/\times 10^{-6}K^{-1}$ |
|---|---|---|---|---|---|
| C | 211 | 13.8 | 4.8 | 8.7 | -0.1 |
| SiC | 350 | 350 | 145 | 145 | 4.5 |
| | $\alpha_T/\times 10^{-6}K^{-1}$ | $\nu_{12}$ | $\nu_{23}$ | $\sigma_c$/MPa | m |
| C | 3.1 | 0.2 | 0.25 | 1780 | 3 |
| SiC | 4.5 | 0.25 | 0.25 | 200 | 2 |

**Table 2** Geometrical parameters in meso-scale

| | $J_s$/mm | $J_w$/mm | $J_h$/mm | $W_w$/mm | $W_h$/mm |
|---|---|---|---|---|---|
| Mean | 4.26 | 1.015 | 0.169 | 1.053 | 0.199 |
| Min | 4.018 | 0.780 | 0.108 | 0.869 | 0.122 |
| Max | 4.703 | 1.539 | 0.225 | 1.25 | 0.261 |

The geometrical parameters in meso-scale are measured from the micrographs; there are 493 groups of parameters obtained. The average, maximum, and minimum value of each parameter is shown in Table 2.

Tables 3 and 4 depict the elastic modulus and the TEC value of 2.5D C/SiC composite from experiments and theoretical models, respectively (Table 5).

By comparison, it can be noticed from these tables that there is a good agreement between theoretical and experimental results. For example, the predicted elastic modulus in warp direction is 147.5GPa, while the experimental result is 138.4GPa, with an error of 6.6 % between predicted and experimental results. And the predicted elastic modulus in weft direction is 121.2GPa, while the experimental one is 113GPa, with an error of 7.3 %. All these excellent comparison results lend compelling support to demonstrate the feasibility of analytical model in analyzing the mechanics properties of 2.5D C/SiC composites.

## 2.5 Uncertainty Analysis of Mechanical Properties

The mechanical properties such as elastic modulus, TEC, and ultimate strength are governed by the properties, geometrical orientation and volume fraction of constituent phases. The stochastic behavior of 2.5D C/SiC composites mechanical properties is detrimental to the composites structures; therefore it is worthwhile to analyze the uncertainty of mechanical properties.

Monte Carlo simulation method has emerged as one of most powerful tools for analysis complex problems, and has been extensively used to predict the future behavior of a system involving basic design variables of known or pre-described probability distributions [14]. Here, three parameters, such as, volume fraction $v_f$, geometrical factor $J_s$, and ultimate strength $\sigma_c$, are selected to carry on the Monte Carlo analysis. Also we assume that these parameters follow the normal distribution, which standard deviations are shown in Table 6.

The probability densities of mechanical and thermal properties along different directions are depicted in Fig. 4. Results show that stochastic behavior of 2.5D C/SiC composites mechanical properties are governed by the stochastic behavior of its components, mechanical properties, and structure of 2.5D composites. When the range of standard deviation of random value becomes small, the dispersion of mechanical properties decreases.

**Table 3** Elastic properties of composite structures from theoretical and experimental analysis

| Warp directions/(GPa) | | | Weft directions/(GPa) | | |
|---|---|---|---|---|---|
| Theoretical value | Experimental value (standard derivation) | Error | Theoretical value | Experimental value (standard derivation) | Error |
| 147.5 | 138.4 (18.0) | 6.6 % | 121.2 | 113 (18.5) | 7.3 % |

**Table 4** TEC of composite structure from theoretical and experimental analysis

| Warp directions/($\times 10^{-6}K^{-1}$) | | | Weft directions/($\times 10^{-6}K^{-1}$) | | |
|---|---|---|---|---|---|
| Theoretical value | Experimental value (standard derivation) | Error | Theoretical value | Experimental value (standard derivation) | Error |
| 1.74 | 1.84 (0.165) | -5.4 % | 1.75 | 1.88 (0.198) | -6.9 % |

## 3 Vane Analysis

### 3.1 Finite Element Model

The first step of vane analysis is to predict the mechanics properties of 2.5D C/SiC composite; then the elastic properties and thermal expansion coefficient (TEC) can be used to analysis the vane structure, and the stress of vane can be evaluated; finally, safety factor is defined as the ratio of strength and the maximum value of stress in vane.

The finite element model of vane is described in Fig. 5a, the principle strain directions of elements are shown in Fig. 5b.

The pressure and temperature distribution of vane are shown in Figs. 6 and 7 [15]. The pressure of inner surface was 0.9 MPa, and the pressure of outer surface was uniformly decreased from 0.8 to 0.68 MPa, pressure decreased as 0.12 MPa. The maximum temperature of the vane is 1126 °C. The stress distribution of vane can be calculated by taking the temperature and pressure loads into the finite element model of vane structure.

Figures 8 and 9 show the stress and deformation distribution of vane, respectively. In this case, the safety factor of vane is 2.1. In order to decrease the mass of vane and increase the reliability of the results, it is necessary to carry out optimization for the vane and then reliability analysis for the optimized results.

### 3.2 Vane Optimization

The multi-objective optimization problem for 2.5D C/SiC composites vane is that the mass of vane and the displacement in radius direction should be minimized, and the safety factor should be greater than certain value such as 1.4, 1.7, 2.0, and 2.3. Volume fraction of fiber, $J_s$ of 2.5D structure, and thickness of vane are selected as design variables. The multi-objective optimization problem for 2.5D C/SiC composites vane is expressed in following equation:

$$\begin{aligned} &\min \text{Mass} = \mathrm{f}_1(vf, Js, Thick) \\ &\min \text{disp} = \mathrm{f}_2(vf, Js, Thick) \\ &\mathrm{S.T.}\,\delta_\sigma \geq 1.4,\ 1.7,\ 2.0 \text{ or } 2.3 \end{aligned} \tag{14}$$

**Table 5** Ultimate strength of composite structure from theoretical and experimental analysis

| | Experimental value (standard derivation) | Theoretical value | Error |
|---|---|---|---|
| Warp direction | 247 (30.1) | 260 | 4.8 % |
| Weft direction | 205 (14.3) | 185 | -9.7 % |

**Table 6** Standard deviation of three key variables

| $v_f$ | *Js*/mm | $\sigma_c$/MPa |
|---|---|---|
| 0.05 | 0.5 | 178 |

where, the range of *vf* is [0.4,0.65], the range of *Js* is [4.2,6.0] mm, the range of thickness is [1.0,3.2] mm.

NSGA2 [16] is adopted to optimize the above-mentioned problem. The optimization results are shown in Table 7. As shown in Table 7, with the increase of the safety factor of the vane, the span of warp yarns and the thickness of vane, the mass of vane and the displacement in radial direction will increase.

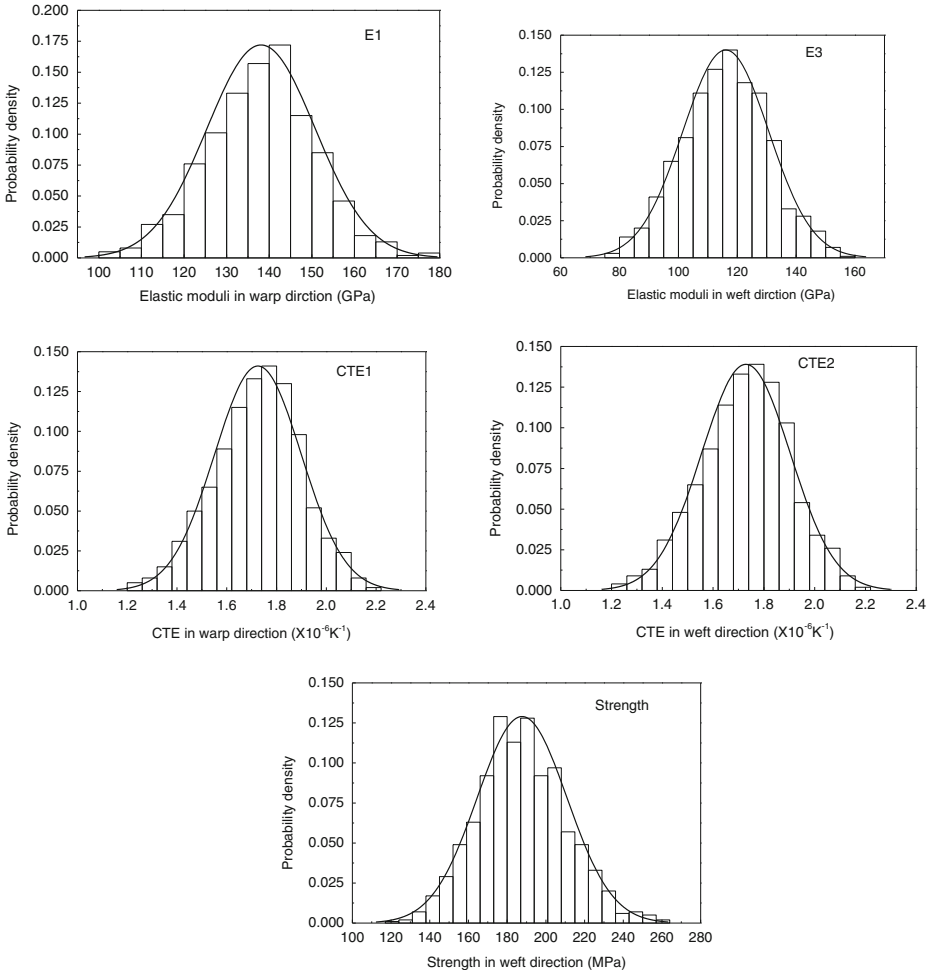


**Fig. 4** Probability density distributions of mechanical and thermal properties of 2.5D C/SiC composite

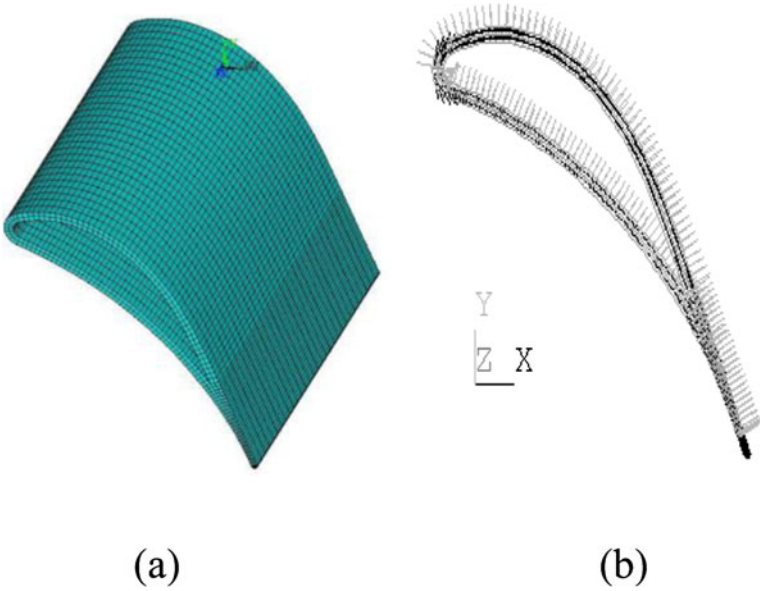


**Fig. 5** Finite element model and mesh generation of turbine stator vane

### 3.3 Reliability Analysis Optimization Results

The manufacture of products often involves a balance between the controllable factors and uncontrollable noise [17]. Murthy [18] shows that due to the deviation of mechanics properties, there is a critical need for reliability analysis is in composites vane. To make sure the safety of structure, the structure strength must be greater than the stress due to the action of loads. A kind of failure probability evaluation model is shown in Fig. 10, $f_S(s)$ is the stress

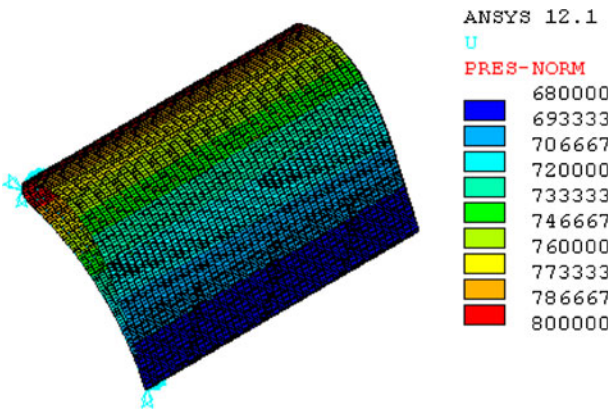


**Fig. 6** Pressure distribution of turbine stator vane

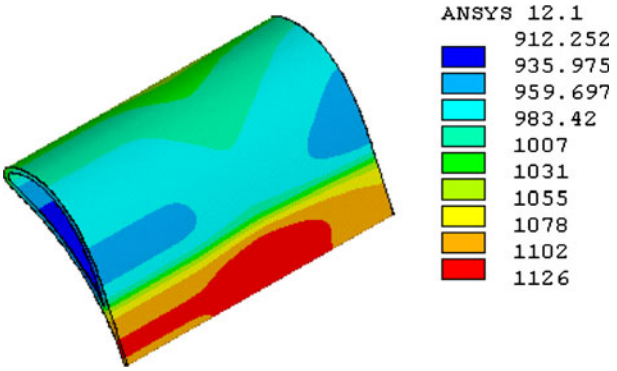


**Fig. 7** Temperature distribution of turbine stator vane

probability of structure, and $f_R(r)$ is the strength probability density of composites materials; their interference area is failure probability.

Four parameters are selected to perform the Monte Carlo analysis, their mean values are shown in Table 7 and their standard deviation is shown in Table 8.

The strength and stress interference of four cases are shown in Fig. 11. It can be noticed that the increase of the thickness of vane decreases the stress of vane and narrow its dispersion.

It is reasonable that reliability of the vane design is dominated by the scatter of random parameters. Figure 12 shows the relationship between reliability and safety factor,

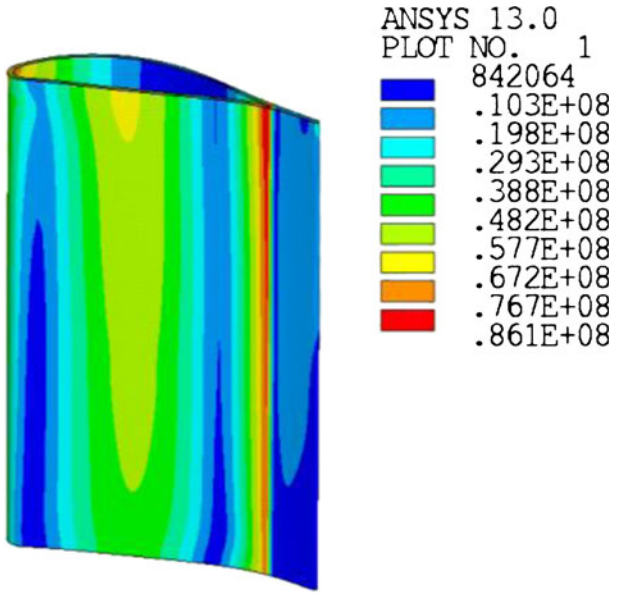


**Fig. 8** Stress distribution of turbine stator vane

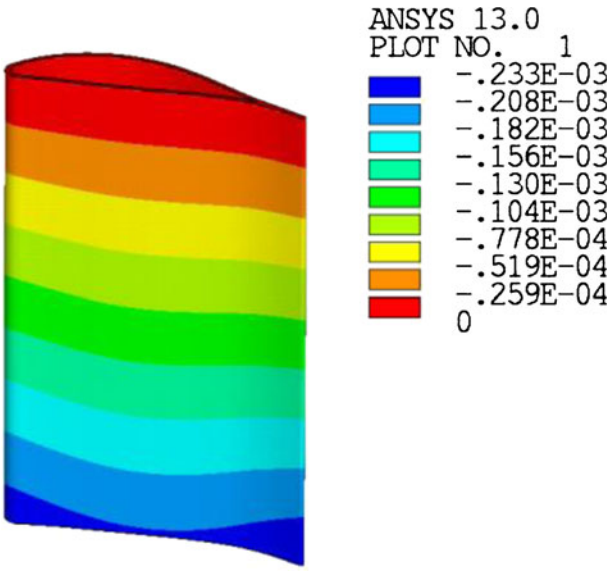


**Fig. 9** Radial deformation of turbine stator vane

where the safety factor increases from 1.4 to 2.3, the reliability increases from 0.833 to 0.998.

## 4 Conclusions

This paper presents a feasible and efficient methodology to design 2.5D C/SiC composites vane system. The following findings have been made:

(1) The micro-structure of 2.5D composite has been studied with the help of optical photomicrographs, and then the architecture of 2.5D composites can be defined by five characteristic parameters. A double-scale model for mechanical properties of 2.5D C/SiC composite has been presented, which can provide a reasonably good correlation with experimental results.

(2) Monte Carlo method has been adopted to investigate the stochastic behavior of 2.5D C/SiC composites mechanical properties controlled by stochastic behavior of components and structure of 2.5D braiding architecture. Results show that the mechanical properties of 2.5D composite follow normal distribution under stochastic component materials mechanical properties and micro-structure parameters.

**Table 7** Optimization results of vane

| Case | $\delta_\sigma$ | $v_f$ | *Js* mm | *Thick*/mm | *Mass*/g | *Disp*/mm |
|---|---|---|---|---|---|---|
| 1 | 1.4 | 0.65 | 5.98 | 1.1 | 24.2 | 0.194 |
| 2 | 1.7 | 0.65 | 5.96 | 1.2 | 26.2 | 0.195 |
| 3 | 2.0 | 0.65 | 5.99 | 1.3 | 27.7 | 0.195 |
| 4 | 2.3 | 0.65 | 6.0 | 1.8 | 36.9 | 0.198 |

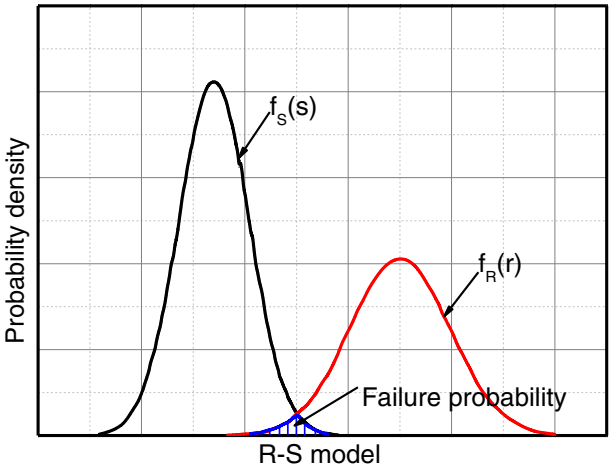


**Fig. 10** Failure probability model

**Table 8** Standard deviation of random variable

| $v_f$ | *Js*/mm | *Thick*/mm | $\sigma_c$/MPa |
|---|---|---|---|
| 0.05 | 0.5 | 0.1 | 178 |

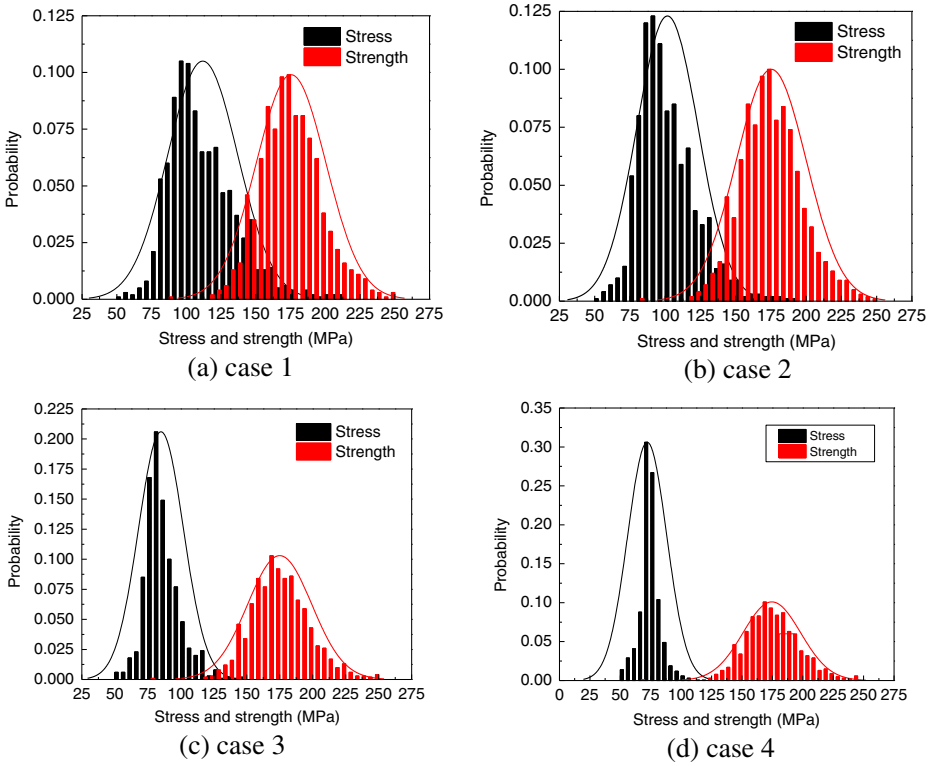


**Fig. 11** Stress-strength interference analyses **a** case 1 **b** case 2 **c** case n case 4

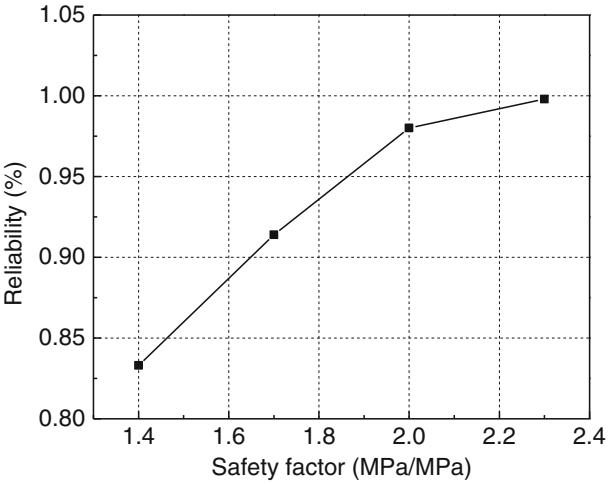


**Fig. 12** Relationship between reliability and safety factor

(3) Vane optimization model is established by combination the analytical model of 2.5D C/SiC composites and the finite element model of vane. Safety factor that affects the results of the optimization was studied. When the safety factor increases, the mass will increase.
(4) The finite element code and probabilistic analysis methods were used to perform the reliability assessment of 2.5D C/SiC composite vane. Results show that the safety factor will increase when the reliability increases. Such methodologies provide an effective method to assess the risk and provide a quantifiable tool to vane design.

**Acknowledgments** Supports of this project provided by National Basic Research Program of China, National Natural Science Foundation of China (51075204), Aeronautical Science Foundation of China (2012ZB52026), Research Fund for the Doctoral Program of Higher Education of China (20070287039), and the Fundamental Research Funds for the Central Universities (NS2014024) are gratefully acknowledged.

## References

1. Dassios, K.G., Aggelis, D.G., Kordatos, E.Z., Matikas, T.E.: Cyclic loading of a SiC-fiber reinforced ceramic matrix composite reveals damage mechanisms and thermal residual stress state. Compos. A: Appl. Sci. Manuf. **44**, 105–113 (2013)
2. Kim, J., Kim, C., Hong, C.: Optimum design of composite structures with ply drop using genetic algorithm and expert system shell. Compos. Struct. **46**(2), 171–187 (1999)
3. Liu, B., et al.: Permutation genetic algorithm for stacking sequence design of composite laminates. Comput. Methods Appl. Mech. Eng. **186**(2–4), 357–372 (2000)
4. Zhao, Q., Ding, Y., Jin, H.: A layout optimization method of composite wing structures based on carrying efficiency criterion. Chin. J. Aeronaut. **24**(4), 425–433 (2011)
5. Eamon, C.D., Rais-Rohani, M.: Integrated reliability and sizing optimization of a large composite structure. Mar. Struct. **22**(2), 315–344 (2009)
6. Puglia, P.D., Sheikh, M.A., Hayhurst, D.R.: Classification and quantification of initial porosity in a CMC laminate. Compos. A: Appl. Sci. Manuf. **35**(2), 223–230 (2004)
7. Dalmaz, A., El Guerjouma, E., Reynaud, P., et al.: Elastic moduli of a 2.5D Cf/SiC composite: experimental and theoretical estimates. Compos. Sci. Technol. **60**(6), 913–925 (2000)

8. Chang, Y., Guiqiong, J., Bo, W., et al.: Elastic behavior analysis of 3D angle-interlock woven ceramic composites. Acta Mechanica Solida Sinica **19**(2), 152–159 (2006)
9. Dong, W.F., Xiao, J., Li, Y.: Finite element analysis of the tensile properties of 2.5D braided composites. Mater. Sci. Eng. A **457**(1-2), 199–204 (2007)
10. Ma, J., Xu, Y., Zhang, L., et al.: Microstructure characterization and tensile behavior of 2.5D C/SiC composites fabricated by chemical vapor infiltration. Scripta Materialia **54**, 1967–1971 (2006)
11. Dong, W.F., Xiao, J., Li, Y.: Finite element analysis of the tensile properties of 2.5D braided composites. Marter. Sci. Eng. A **457**, 199–204 (2007)
12. Stawovy, R.H., Kampe, S.L., Curtin, W.A.: Mechanical behavior of glass and Blackglas® ceramic matrix composites. Acta Mater. **45**(12), 5317–5325 (1997)
13. Curtin, W.A.: Ultimate strengths of fibre-reinforced ceramics and metals. Composites **24**(2), 98–102 (1993)
14. Jeong, H.K., Shenoi, R.A.: Probabilistic strength analysis of rectangular FRP plates using Monte Carlo simulation. Comput. Struct. **76**(1-3), (2000)
15. Sun, J.: Integrated design optimization of structure and material of braided composites. Nanjing University of Aeronautics and Astronautics, NanJing (2010)
16. Deb, K., Pratap, A., Agarwa, S., et al.: A fast elitist multiobjective genetic algorithm: NSGA-II. IEEE Trans. Evol. Comput. **6**(2), 182–197 (2002)
17. Lee, M.C.W., Payne, R.M., Kelly, D.W., et al.: Determination of robustness for a stiffened composite structure using stochastic analysis. Compos. Struct. **86**(1–3), 78–84 (2008)
18. Murthy, P.L.N., Nemeth, N.N., Brewer, D.N., et al.: Probabilistic analysis of a SiC/SiC ceramic matrix composite turbine vane. Compos. Part B **39**(4), 694–703 (2008)